

Spectral Analysis of Infrared Lamps for Use in the High Speed Sintering Process

Farhana Norazman*, Patrick Smith* and Neil Hopkinson†

*Department of Mechanical Engineering, The University of Sheffield, Sheffield S1 3JD, UK

†Xaar plc, 316 Science Park, Milton Road, Cambridge CB4 0XR, UK

Abstract

High Speed Sintering (HSS) is an additive manufacturing (AM) process that utilizes a combination of inkjet printing and infrared heating to create three dimensional objects from polymer powder. The interaction between the ink, sintering lamp and powder is pivotal in promoting the optimum sintering behavior required to ensure the high dimensional accuracy and strength of parts. This paper investigates the relationship between the spectral irradiance of sintering lamps and the mechanical properties of high speed sintered parts. Nylon-12 parts were manufactured using two different infrared lamps. Ultimate tensile strength, Young's modulus and elongation at break of the manufactured parts were determined. Densities of parts were calculated while porosities were measured using micro-computed tomography. Irradiances of the IR lamps were measured and their spectra analyzed. Results show that the parts manufactured using the high irradiance lamp had better tensile properties, and lower density and porosity compared to the low irradiance lamp.

Introduction

High Speed Sintering (HSS) process is a combination of powder bed fusion and binder jetting [1]. The process employs an inkjet print head to deposit radiation-absorbing ink over a powder build bed with an infrared lamp as the heat source [2, 3]. See Figure 1 for HSS process.

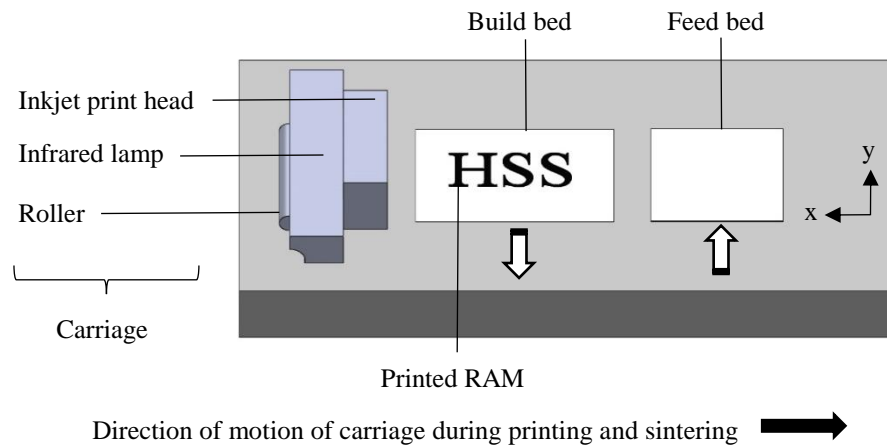


Figure 1: High speed sintering process

The main components; the inkjet print head, infrared (IR) lamp and roller are contained in a moving carriage. At the start of a build, the feed bed is raised by a layer thickness and polymer powder is deposited onto the build bed as the roller traverses across the bed. The infrared lamp radiates heat over the powder-filled build bed in the preheat stage. As the carriage returns, the build bed is lowered and monochromatic bitmap images are printed over the build bed in Radiation Absorbent Material (RAM). The infrared lamp provides instantaneous radiation over the whole bed and the RAM absorbs sufficient thermal energy to selectively sinter the underlying powder. Surrounding powder will remain unsintered and act as a support.

Studies have shown that the mechanical properties of polymer AM parts, in particular the ultimate tensile strength, Young’s modulus and elongation at break are comparable but still inferior in relation to injection molded parts [4]. This can be attributed to the difference in binding mechanisms or insufficient thermal energy input in AM. The latter issue is the focal point of this paper, through an investigation of irradiance. Irradiance of radiation is a measure of the radiation falling on a surface, defined as the energy falling on a surface per unit time. The irradiance follows the inverse square law $I = k/d^2$ where I is irradiance, k is constant and d is the distance measured from the source.

One of the few disadvantages of the polymer powder bed sintering process is high porosity in parts, which is largely due to the capillary spreading action of a liquid upon melting. Porosity is expressed as the fraction of void over the total volume [5]. The porosity of AM parts have previously been investigated using micro computed tomography or relative density method, alongside its effect on mechanical properties [6-9]. Literature on HSS is limited and highly focused on the mechanical properties of parts. A number of studies have investigated the sintering behaviour in the HSS process as a function of powder bed temperatures and IR lamp power levels [10, 11]. The relationship between the level of carbon black absorber in the ink and parts mechanical properties has been studied by varying the print density or adopting an alternative ink composition [12, 13]. The standard material which has been used in the HSS process is nylon-12 with a melt temperature of 186°C.

Experimental Methodology

This section details the experimental methodology used in this study. HSS parts were manufactured using two different infrared lamps. Manufactured parts were tensile tested and the ultimate tensile strength, Young’s modulus and elongation at break were obtained and compared. Part dimensions were measured and their densities were calculated. Porosities were investigated using micro-computed tomography. The lamps were measured for irradiance and spectral analysis was carried out.

Manufacturing of high speed sintering parts

Two sintering lamps were used in this study; Lamp 1 and Lamp 2. Both lamps were commercially available 2 kW quartz halogen infrared lamps with a difference in reflector coating. All parts were printed at a constant print density of 4,500 pL/mm². 100% virgin nylon-12 powder was used to manufacture the parts. The parts were oriented on the XY plane and processed on the HSS machine using a set of standard build parameters as listed in Table 1.

Table 1: High speed sintering build parameters

Build bed overhead temperature	Build bed jacket temperature	Feed bed overhead temperature	Feed bed jacket temperature	Preheat lamp power & speed	Sintering lamp power & speed
156°C	166°C	120°C	140°C	1 kW (50%) at 150 mm s ⁻¹	2 kW (100%) at 120 mm s ⁻¹

Two replica builds were set for each lamp configuration using the same build parameters. Each build consisted of six ASTM type IV tensile test specimens and three rectangular blocks. The dimensions were 115 x 19 x 3.2 mm for the tensile specimens and 40 x 10 x 3.2 mm for the blocks. The manufactured parts are demonstrated in Figure 2.

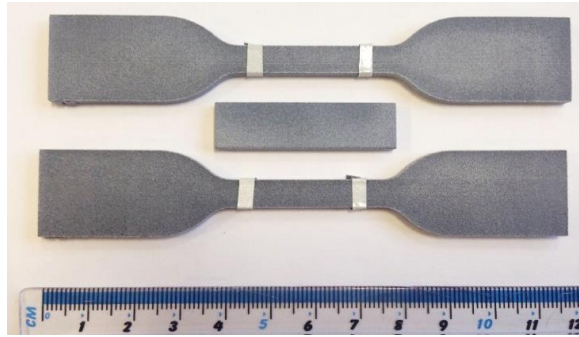


Figure 2: High speed sintered parts

Tensile testing

Tensile testing was conducted on a Tinius Olsen H5KS tensile test machine equipped with an H500L laser extensometer. The test was performed according to the ASTM D638 standard under 5 kN load at a crosshead speed of 5 mm/min for all specimens.

Density measurement

The apparent density of each rectangular part was determined using the following formula: density, $\rho = \text{mass, } m / \text{volume, } v$. The mass was obtained using an Ohaus Pioneer PA64C balance ± 0.0001 g and the volume was calculated from the linear dimensional measurements obtained using a Vernier calliper ± 0.01 mm. Five measurements were taken for each specimen and an average value was calculated.

Micro-computed tomography (micro-CT) scan

3D structures of the high speed sintered parts were evaluated via micro-CT. The rectangular parts were mounted in a Skyscan 1172 scanner, where sections of 5mm x 10mm x 3.2mm were scanned. The scanning parameters used were as following; 148 μ A current, 41kV voltage, 6 μ m pixel size, 360 $^\circ$ scan rotation and 7 $^\circ$ rotation step. Porosities were calculated from the reconstructed images of each specimen.

Spectral irradiance measurement

The irradiances of the two infrared lamps (Lamp 1 and Lamp 2) were measured between 300–2,500 nm wavelength range. Figure 3 illustrates the plan view of the test setup.

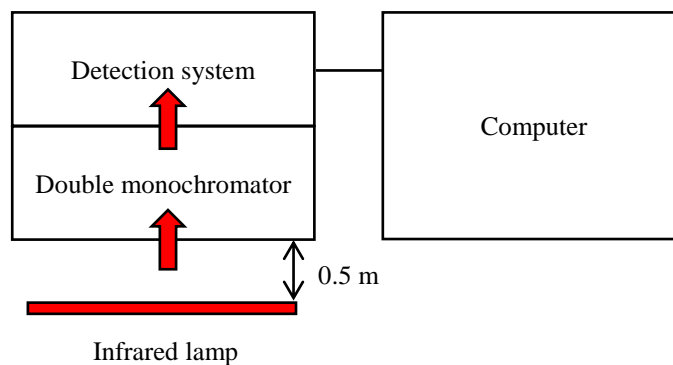


Figure 3: Plan view of irradiance measurement setup

The irradiances of the IR lamps were measured at a distance of 500 mm parallel to, and along the optical axis of the measurement plane. Light was collected from the lamp under test using a Bentham D7 cosine response diffuser ($f2 < 1\%$) attached to a randomised fibre bundle, coupled to a monochromator for spectral analysis. The monochromator used was a Bentham DM150 double monochromator, fitted with 600 and 1200 lines/mm gratings; a measurement bandwidth of 5nm was employed throughout the spectral range. The detection system comprised a silicon detector used over the range 300–1,100 nm range and a Pyroelectric detector used over the range 1,000–2,500 nm, providing some overlap to check for continuity.

The irradiance data from 300–2,500 nm was based on a PTB (Germany) traceable calibrated quartz halogen lamp. Figure 4 compares the spectral distribution of tested Lamp 1 and Lamp 2 over the infrared region.

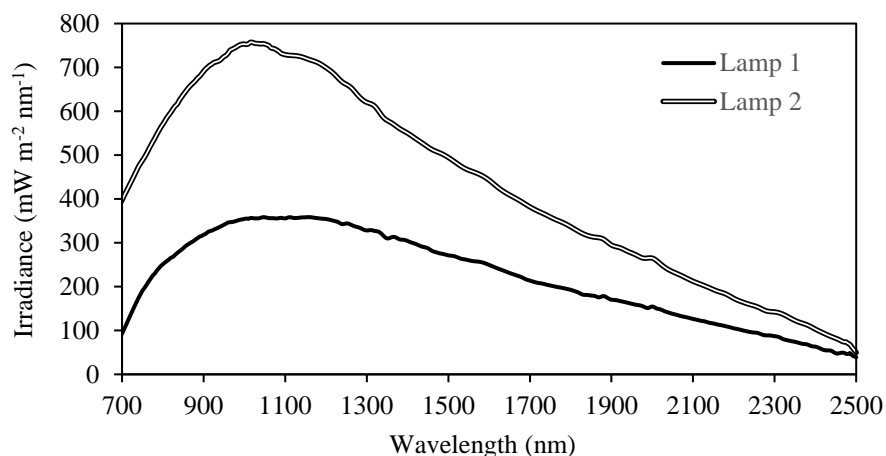


Figure 4: Spectral output of the infrared lamps

Figure 4 shows how the difference in the reflector coating resulted in a difference in irradiance. The irradiance of Lamp 2 is higher than Lamp 1, with its peak irradiance twice as high as Lamp 1. The irradiance peaks are at 1,045 nm and 1,020 nm in the near infrared region for Lamp 1 and Lamp 2, respectively. The total irradiance over this wavelength range is 398 Wm^{-2} and 770 Wm^{-2} for Lamp 1 and Lamp 2 respectively. This indicates that Lamp 2 radiates almost double the energy than Lamp 1 when applied over the same area and exposure time.

The uncertainty in the spectral irradiance and radiance measurements was estimated not to exceed $\pm 5\%$ over the whole spectral range, based on uncertainty in the calibrated standard and in the repeatability of the measurement.

Results and Discussion

Tensile properties

The effects of the lamp irradiance on the tensile properties of high speed sintered parts are demonstrated in Figures 5 – 7. Figure 5 compares the ultimate tensile strength values between the two sets of builds.

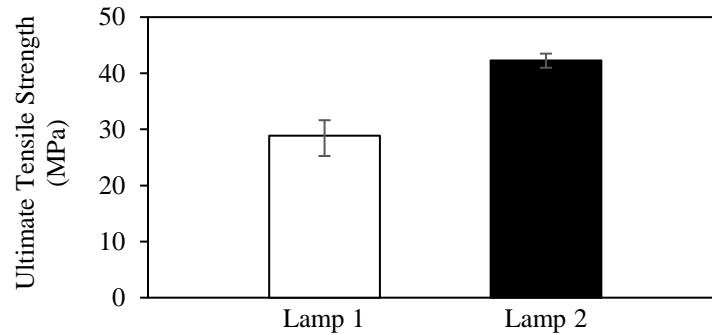


Figure 5: Ultimate tensile strength of high speed sintered parts

Parts manufactured using the low output Lamp 1 had a lower average tensile strength of 28.8 MPa in contrast to 42.2 MPa of high output Lamp 2. Previous study has shown that a higher infrared power level causes a higher level of sintering of powder [11]. A difference in lamp power level is comparable to a difference in irradiance as a function of thermal energy input, thus similar effects were to be expected in this study. From Figure 4, it was therefore expected that Lamp 2 enabled greater degree of sintering and produced stronger parts. These parts' tensile strength were also reasonable as the material supplier EOS quoted a tensile strength value of 48 MPa for laser sintered nylon-12 parts [14].

Figure 6 illustrates the effect of irradiance on the Young's modulus of the high speed sintered parts.

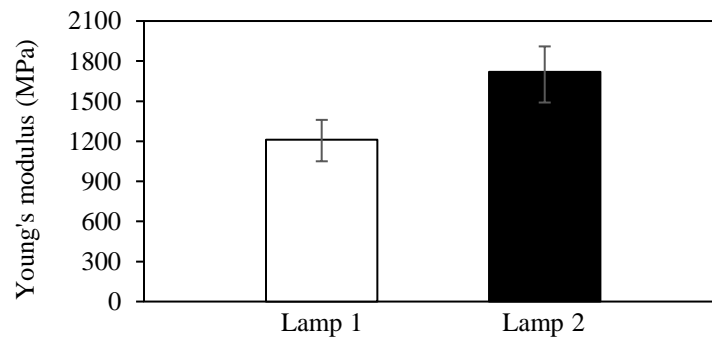


Figure 6: Young's modulus of high speed sintered parts

It can be seen that a 100% increase in irradiance leads to a 50% increase in modulus. An average modulus of 1212 MPa was observed for Lamp 1 versus 1720 MPa for Lamp 2 parts. These were slightly superior compared to EOS's quoted value of 1650 MPa [14].

Figure 7 compares the elongation at break values for high speed sintered parts fabricated using the two lamp configurations.

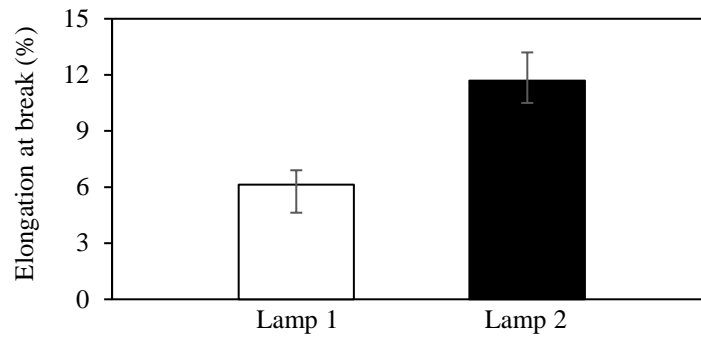


Figure 7: Elongation at break of high speed sintered parts

A similar trend can be observed for elongation at break, where the tensile specimens failed at an average of 6.1% and 11.7% elongation for Lamp 1 and Lamp 2, respectively.

Density and porosity

The apparent densities of parts fabricated by Lamp 1 were measured at 0.901 – 0.928 g/cm³. The densities of parts fabricated by Lamp 2 were measured higher at 0.974 – 0.993 g/cm³. This suggests that the increase in thermal input contributes to a 7% increase in densification, which further leads to improvement in tensile properties. Previous work has reported the density of a laser sintered and injection molded nylon-12 part to be 0.960 g/cm³ and 1.030 g/cm³ respectively [15].

Figure 8 shows the cross-sectional images of two parts manufactured using Lamp 1 and Lamp 2 as seen on micro-CT.

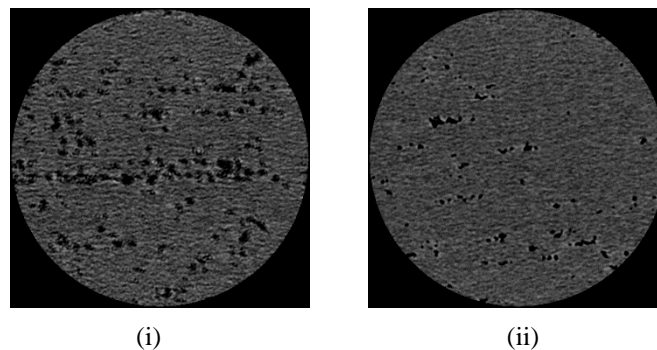


Figure 8: Cross-sectional images of high speed sintered parts manufactured by (i) Lamp 1 and (ii) Lamp 2

It can be seen that the part manufactured using Lamp 2 (on the right) contained less void and was less porous than Lamp 1. The average porosity measured for Lamp 1 parts was 12% compared to 2% for Lamp 2. In comparison, laser sintered nylon-12 parts were reported to have a porosity range of 2.5 – 5.0% when manufactured at a range of energy density levels [6]. The positive correlation between the density and porosity values suggests that the apparent part density can potentially be used to estimate the level of porosity in parts.

Conclusions

The aim of this study was to quantitatively correlate irradiance values with the mechanical properties of high speed sintered parts. The results showed a significant enhancement in tensile properties, density and porosity with an increase in irradiance.

Lamp 2 was more preferable to use at this set of parameters as it provided sufficient energy needed for optimum sintering, while parameters optimization will be needed to maximise the output of Lamp 1. A high energy output was generally better to ensure sufficient energy input to the carbon black particles in the ink. However, there was a trade-off between strength and accuracy as too much thermal energy can either sinter unprinted surrounding powder or degrade the part.

The spectral output of a sintering lamp can provide an understanding of its suitability to use in the HSS process. The results from this study can be used to benchmark the selection of sintering lamp in the future, including considerations of lamp geometry, design or coating material.

References

1. Wohlers Associates 2015. The future of additive manufacturing. *Wohlers Report 2015: 3D Printing and Additive Manufacturing State of the Industry Annual Worldwide Progress Report*. Colorado: Wohlers Associates Inc.
2. Hopkinson, N. & Erasenthiran, P. 2004. High Speed Sintering – Early Research into a New Rapid Manufacturing Process. 2004 Austin, Texas. The University of Texas at Austin, 312 - 320.
3. Thomas, H. R., Hopkinson, N. & Erasenthiran, P. 2006. High Speed Sintering - Continuing research into a new Rapid Manufacturing process. 2006 Austin, Texas. The University of Texas at Austin, 682-691.
4. Kruth, J. P., Levy, G., Klocke, F. & Childs, T. H. C. 2007. Consolidation phenomena in laser and powder-bed based layered manufacturing. *CIRP Annals - Manufacturing Technology*, 56, 730-759.
5. German, R. M. 1996. *Sintering theory and practice*, New York ; Chichester, Wiley.
6. Dewulf, W., Pavan, M., Craeghs, T. & Kruth, J.-P. 2016. Using X-ray computed tomography to improve the porosity level of polyamide-12 laser sintered parts. *CIRP Annals - Manufacturing Technology*, 65, 205-208.
7. Rouholamin, D. & Hopkinson, N. 2016. Understanding the efficacy of micro-CT to analyse high speed sintering parts. *Rapid Prototyping Journal*, 22, 152-161.
8. Athreya, S. R., Kalaitzidou, K. & Das, S. 2011. Mechanical and microstructural properties of Nylon-12/carbon black composites: Selective laser sintering versus melt compounding and injection molding. *Composites Science and Technology*, 71, 506-510.
9. Hitt, D. J., Haworth, B. & Hopkinson, N. 2011. Fracture mechanics approach to compare laser sintered parts and injection mouldings of nylon-12. *Proceedings of the Institution of Mechanical Engineers, Part B: Journal of Engineering Manufacture*, 225, 1663-1672.
10. Majewski, C. E., Hobbs, B. S. & Hopkinson, N. 2007. Effect of bed temperature and infra-red lamp power on the mechanical properties of parts produced using high-speed sintering. *Virtual and Physical Prototyping*, 2, 103-110.

11. Majewski, C. E., Oduye, D., Thomas, H. R. & Hopkinson, N. 2008. Effect of infra-red power level on the sintering behaviour in the high speed sintering process. *Rapid Prototyping Journal*, 14, 155-160.
12. Ellis, A., Noble, C. J. & Hopkinson, N. 2014. High Speed Sintering: Assessing the influence of print density on microstructure and mechanical properties of nylon parts. *Additive Manufacturing*, 1, 48-51.
13. Fox, L., Ellis, A. & Hopkinson, N. 2015. Use of an Alternative Ink in the High Speed Sintering Process. *In: Proceedings of the 26th Solid Freeform Fabrication Symposium*, 2015 Austin, Texas. The University of Texas at Austin, 456-463.
14. EOS. 2010. *EOS material data sheet for PA2200* [Online]. Available: <http://eos.materialdatacenter.com/>.
15. Ajoku, U., Hopkinson, N. & Caine, M. 2006. Experimental measurement and finite element modelling of the compressive properties of laser sintered Nylon-12. *Materials Science and Engineering: A*, 428, 211-216.